Three-dimensional shape analysis of coarse aggregates: New techniques for and preliminary results on several different coarse aggregates and reference rocks

by

S.T. Erdogan [a], P.N Quiroga [a], D.W. Fowler [a] , H.A. Saleh [b], R.A. Livingston [b], E.J. Garboczi [c], P,M. Ketcham [d], J.G. Hagedorn [d], S.G. Satterfield [d]

[a] Department of Civil Engineering, University of Texas, Austin

[b] Turner-Fairbank Research Center, Federal Highway Administration, Mclean, VA

[c] Building and Fire Research Laboratory National Institute of Standards and Technology, Gaithersburg, MD

[d] Mathematical and Computational Sciences Division, National Institute of Standards and Technology, Gaithersburg, MD

NIST

National Institute of Standards and Technology
Technology Administration, U.S. Department of Commerce

Cement and Concrete Research

ELSEVIER

Three-dimensional shape analysis of coarse aggregates: New techniques for and preliminary results on several different coarse aggregates and reference rocks

S.T. Erdogan [a], P.N. Quiroga [a], D.W. Fowler [a], H.A. Saleh [b], R.A. Livingston [b], E.J. Garboczi [c,*], P.M. Ketcham [d], J.G. Hagedorn [d], S.G. Satterfield [d]

[a] Department of Civil Engineering, University of Texas, Austin, TX 78712, USA
[b] Turner-Fairbank Research Center, Federal Highway Administration, McLean, VA 22101, USA
[c] Materials and Construction Research Division, National Institute of Standards and Technology, Gaithersburg, MD 20899, USA
[d] Mathematical and Computational Sciences Division, National Institute of Standards and Technology, Gaithersburg, MD 20899, USA

Abstract

The shape of aggregates used in concrete is an important parameter that helps determine many concrete properties, especially the rheology of fresh concrete and early-age mechanical properties. This paper discusses the sample preparation and image analysis techniques necessary for obtaining an aggregate particle image in 3-D, using X-ray computed tomography, which is then suitable for spherical harmonic analysis. The shapes of three reference rocks are analyzed for uncertainty determination via direct comparison to the geometry of their reconstructed images. A Virtual Reality Modeling Language technique is demonstrated that can give quick and accurate 3-D views of aggregates. Shape data on several different kinds of coarse aggregates are compared and used to illustrate potential mathematical shape analyses made possible by the spherical harmonic information.
© 2006 Elsevier Ltd. All rights reserved.

Keywords: Image and shape analysis; Aggregate; Composite; Modeling

1. Introduction

Mathematical (spherical harmonic series) and experimental (X-ray computed tomography) techniques to characterize the particle shape of aggregates used in concrete have been demonstrated [1], and a general case has been made for the important effect on composite properties of inclusion particle shape [2–5]. In concrete, the rheology of fresh concrete and the mechanical properties of early-age concrete are quite sensitive to aggregate shape, because of the large contrast in rheological and elastic properties between the matrix and the aggregates [4,6]. But acquiring true, full three-dimensional (3-D) particle shape information via X-ray computed tomography (CT) is not

an easy task [7]. The purpose of this paper is to clearly describe successful techniques for acquiring and processing this kind of information, and then showing how it can be used in the study of several different kinds of aggregates. This paper can be viewed as a sequel to Garboczi [1], systematically improving and further applying the experimental and numerical techniques that were pioneered in that paper.

For example, the sample preparation techniques needed for successful imaging of particles in 3-D are not trivial. In this paper, guidelines for sample preparation and image analysis and reconstruction are described. Uncertainty analysis of the spherical harmonic mathematical procedure has been previously carried out using analytically smooth ellipsoidal particles, but not on real aggregate shapes. In the present paper, the spherical harmonic/X-ray CT procedure is further validated using real rocks. Visualization of images that have been reconstructed from the spherical harmonic series process has been previously

* Corresponding author.
E-mail address: edward.garboczi@nist.gov (E.J. Garboczi).

made [1] using a ray-tracing program specialized to mainly Unix and Linux machines and so not easily accessible to the average materials science researcher. Virtual Reality Modeling Language (VRML) procedures are now shown to be able to generate images that can be easily visualized and manipulated on popular web browser software. Finally, novel shape analysis procedures, made possible by the spherical harmonic series information, are applied to four different kinds of coarse aggregates. The results are used to show how analysis of shape data can be done, to show what kinds of shape analyses are now possible, to connect to more empirical measures of particle shape, and to suggest application possibilities for the effect of aggregate particle shape on concrete properties like fresh concrete rheology and early-age mechanical properties. These kinds of experimental/numerical techniques can also be used to generate mathematical models of aggregates that can be directly incorporated into software packages like the Virtual Cement and Concrete Testing Laboratory [8] and there used to construct concrete models and help predict concrete properties.

2. Mathematical background

The spherical harmonic mathematical analysis of particle shape relies on Eq. (1), which states that any sufficiently smooth function $r(\theta,\phi)$, where θ and ϕ are the azimuthal and polar angles of 3-D spherical coordinates, can be written as a series of spherical harmonic functions [1], where the Y_{nm} are the complex spherical harmonic functions and the a_{nm} are complex coefficients.

$$r(\theta,\phi) = \sum_{n=0}^{N} \sum_{m=-n}^{n} a_{nm} Y_{nm}(\theta,\phi) \qquad (1)$$

Strictly speaking, the series in Eq. (1) becomes exact only as $N \rightarrow \infty$. However, like 2-D Fourier series, a finite value of N is usually found to give an adequate approximation of a given function, within some specified uncertainty limit. There are other mathematical approaches to analyzing particle shape that have been extensively discussed [9].

In the case of aggregates used in concrete, the function $r(\theta,\phi)$ gives the distance from the centroid (equal to the center of mass for a uniform density object) to a given point on the surface of the particle, in a direction specified by the two angles θ (latitude) and ϕ (longitude). Using a numerically determined $r(\theta,\phi)$ function from a 3-D image, in this case derived from X-ray CT, one can sometimes accurately determine coefficients up to $N=40$ or so coefficients, but $N=12-20$ can usually satisfactorily represent the particle shape [1].

Fig. 1 focuses on reference rock number 1. Each 2-D image, taken from a 3-D VRML image, shows what the spherical harmonic reconstruction looks like, in approximately the same orientation, for a different number of spherical harmonic coefficients. The simplest shape, shown in the top left hand corner of Fig. 1, is simply a sphere and uses only the a_{00} coefficient ($N=0$). Using all the coefficients up to $N=2$ is mathematically equivalent to an ellipsoid [10]. In the bottom right hand corner, just before a digital camera image of the real

Fig. 1. This figure shows a series of 2-D images taken from the VRML particle reconstruction of reference rock 1. From top left to bottom right, the highest order of spherical harmonic coefficients used (value of N in Eq. (1)) was 0, 2, 4, 6, 9, 12, 15, 18, and 40. The final image on the bottom right is a digital camera image of the real rock, in the same orientation, about 80 mm in length in the vertical direction.

rock, coefficients up to $N=40$ were used to create the computational image. The shape complexity of the images increases as a larger number of coefficients are used. Fig. 1 shows that using spherical harmonics up to about $N=15$ captures the basic shape of the rock, while using values of N larger than 15 brings out smaller details of the shape and texture.

3. Sample preparation, image analysis, and VRML image production

The sample preparation needed for usable X-ray CT images to be obtained has several requirements. First, the samples must be mechanically stable, as they have to be handled and placed into the X-ray CT scanner and rotated slowly, sometimes for periods of hours [7]. It is necessary to embed the particle or particles in a matrix of suitable density that can be molded into a cylinder, which makes the 2-D image reconstruction algorithm more efficient. Second, in order to be able to pick out aggregates both from the matrix material and from each other, one must have: (1) a matrix material that differs significantly in X-ray absorption characteristics from the aggregates and (2) aggregates that do not touch spatially. Requirement (1) ensures an adequate contrast between aggregates and matrix, so that each 2-D image slice can be properly thresholded to isolate the aggregates. Requirement (2) is necessary so that aggregates can be separately identified computationally, as aggregates that are touching appear to form one particle, which will contribute to error in the shape analysis.

For requirement (1), we have found that a packed dry cement matrix or an ordinary cement paste matrix can be used with solid coarse (coarse=size larger than 5 mm) aggregates (nominally non-porous) and will give sufficient contrast. A
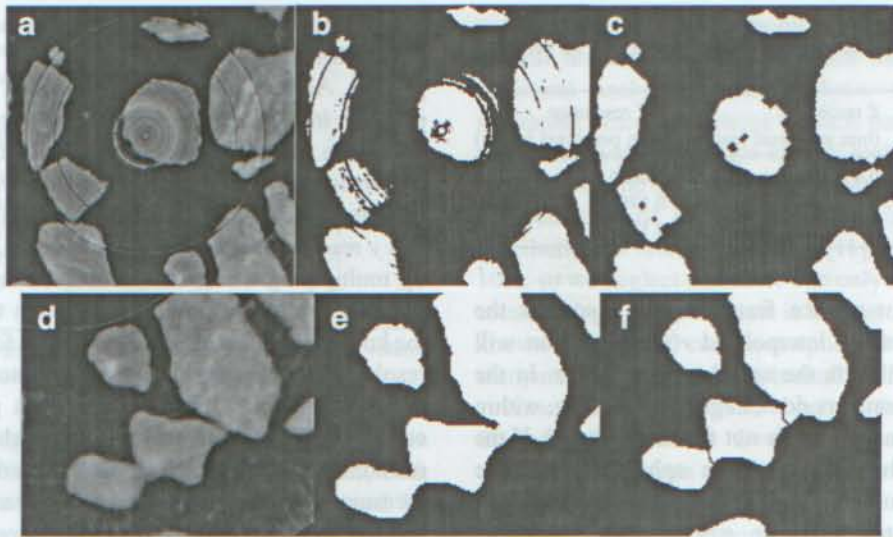
Fig. 2. Illustrating (a) part of a gray scale image taken directly from X-ray CT, (b) the same part but thresholded, showing ring artifacts, (c) the same image after closing/opening, leaving behind some interior porosity that will be removed at a later stage, (d) a different part of the original image, (e) the same image after segmentation and closing/opening, and (f) the same image after limited watershed splitting operations have been performed. In (f), the thin black lines just separate the particles. Each image is about 25 mm^2.

simple paraffin wax matrix can also work well for coarse aggregate, with hand placement of particles [11]. An epoxy matrix works better for fine (fine=size less than 5 mm) aggregates. Requirement (2) is harder to realize. For mortar matrices surrounding coarse aggregates, we used volume fractions of coarse aggregates that were more dilute than is typically specified for concrete, about 20%. In these cases, aggregates were still frequently touching in the resulting images. Either a more dilute quantity should be used, or else a more regular dispersion, by hand, should be carried out, to make sure that aggregates are not touching in 3-D. But even the best physical dispersion will result in some apparent aggregate touching in the X-ray CT images. When images are reconstructed from the original X-ray scans, the limited spatial resolution can often create a "blurring effect" that causes particles that lie close together physically to become touching in the CT images [7], since only matrix distances greater than 1 voxel in size can be resolved. Also, when one thresholds the images to isolate the aggregates, inevitably there is some misclassification of the edges of particles that cause some artificial particle touches. In this case, image analysis techniques become important.

Consider the output from the X-ray CT scan of a single cylindrical sample, 50 mm in diameter and 100 mm high. If a 512×512 image is used, as was done in our case, then the resolution would be 50 mm per 512 pixels=97.7 μm per pixel, if the cylinder diameter fit exactly into the square image. If the same resolution were used in the vertical direction, then there would be 1024 slices generated, each 97.7 μm thick. In these 1024 images, many or most images have touching particles. A quick visual scan by a trained operator can easily identify particles that are touching and manual image processing procedures can be used to separate the two particles with a minimal loss of information. However, this is impractical to do for all the 1024 images resulting from one sample. There can

also be "ring" type artifacts that appear as concentric circular "ripple marks" in each slice (Fig. 2a). When one thresholds images, this can result in thin black rings going through the white aggregates (Fig. 2b). We have found that these are quite easy to remove using a "closing/opening" sequence of operations [12], which leaves the original particles nearly unchanged while removing these thin black rings. Fig. 2c gives the result of a closing/opening operation on the image of Fig. 2b.

Fortunately, image processing can be readily automated. Separating particles can be done through a technique called "watershed splitting", which is a technique of controlled erosion and dilation so that particles, once split by erosion, do not come together again via dilation [12]. We emphasize that the image analysis step usually does cause some small loss of information and a corresponding increase in particle shape uncertainty. Fig. 2d shows a different part of the same original image as that used in Fig. 2a. Fig. 2e shows this image after segmentation and closing/opening and Fig. 2f shows the resultant image after limited watershed splitting. Clearly some artifacts remain or have been caused by the image analysis operation (e.g., small appendages on particles), but these are minimal, changing particle volumes and surface areas only on the order of a few percent.

Once the individual 3-D particles have been built by stacking up clean 2-D images, one must also eliminate small internal pores that are probably due to the thresholding process or that might have been a real part of the aggregates. Small internal pores in a 3-D particle can be identified with a modified burning algorithm and eliminated. Leaving them in the particle will introduce gross errors when the spherical harmonic coefficients are computed [1].

There must be error-checking steps in the $r(\theta,\phi)$ function construction process. If by chance two particles have been "welded" into one, it will almost certainly have an odd shape

Table 1
Volume (measured by Archimedes' method) and resolution data for reference rocks

Rock number	Measured volume (10^4 mm³)	Z resolution (mm per voxel length)	X,Y resolution (mm per voxel length)
1	4.78±0.04	0.4	0.0626
2	6.05±0.04	0.5	0.1908
3	2.82+0.04	0.5	0.1985

and probably re-entrant surface features [1,11], so that the volume calculated from the interpolated $r(\theta,\phi)$ function will probably not agree well with the actual voxel volume. In the program, if these two numbers do not agree closely, e.g. within 3%, the particle is discarded and is not further analyzed. If the interpolation passes this test, and the spherical harmonic coefficients are obtained, then the Gaussian curvature is computed and integrated over the surface of the particle. Normalized by $1/4\pi$, this integral must be equal to unity for a closed surface [1], thus serving as an additional error check on how accurately the particle is approximated by spherical harmonic coefficients. If the computed Gaussian curvature differs from unity by more than a small amount, e.g. 5%, before $N \approx 14$, then the particle shape representation is judged to have something wrong with it and the particle is not further analyzed. The value of $N=14$ was judged to be a minimum number of coefficients required to adequately represent the shape of a real aggregate. Also, particles that are too small are not analyzed. We tend to use a cutoff of 1000 voxels, since having roughly 10 voxels in each direction will give an adequate digital representation of true shape. If there is not an adequate digital representation in the X-ray CT image, then the spherical harmonic representation will not be adequate either. Previously [1], we said that 5 voxels in each direction would be sufficient, with a volume cutoff of 125 voxels, but after more experience, it appears that a larger number is required.

Virtual Reality Modeling Language (VRML) [13] is a simple language for specifying 3-D shapes by giving a grid of points on the surface and specifying how these nodes are grouped into polygons. A VRML browser, available in several forms as a plug-in for common HTML web browsers, allows one to see a 3-D rendering of the object, and rotate, expand, shrink, and translate it using a mouse. Having the set of spherical harmonic coefficients, which define the particle shape analytically, one can readily generate a grid of points on the surface of an aggregate image specified by their Cartesian coordinates and their connectivity to neighboring points. With the addition of a few special commands, a VRML image file can be automatically generated by the same program that calculates the spherical harmonic coefficients.

4. Reference rocks

For direct comparison of mathematical analysis and experimental measurement, we used three arbitrary reference rocks that we could image using the X-ray CT, and then remove from the sample to be able to measure in other ways and compare with the VRML image. Rock 1 was shown in Fig. 1;

rocks 2 and 3 were more flat and rough than was rock 1, giving a more stringent test on the spherical harmonic generation process. All three rocks were embedded in dry, packed cement powder in cylindrical samples. To precisely identify the resolution of the non-cubic voxels in the X-ray CT images, the volumes of the three rocks were measured using Archimedes' method of weighing in air and in water. The x and y resolutions of the images for each rock were determined by multiplying the actual number of voxels, N, in the image times the volume of each voxel, which was ZXY, where Z was the known z-resolution and $X=Y$ stands for the unknown x and y resolutions, which are always equal. Since the physical volume, V, of the sample is known to a high precision, one simply equates $V=NZX^2$ and solves for X. Table 1 shows the actual resolutions used for each of the standard rocks, along with the measured volumes. In more modern machines, this step is not needed and the voxel size in all three directions is known independently [11].

ASTM D4791 [14] defines the length (L) of an aggregate as the maximum distance between two surface points. The width (W) is defined as the longest surface–surface distance that is perpendicular to the length, and the thickness (T) is the largest surface–surface distance that is perpendicular to both L and W. These values were numerically computed from the spherical harmonic series with an uncertainty of 1.0 mm, since there is no exact equation for these numbers. The values of L, W, and T were measured directly on the reference rocks using digital calipers. The calipers have an intrinsic uncertainty of 0.1 mm, but the actual uncertainty in measuring L, W, and T is larger, about 2.0 mm, since it is dominated by being able to estimate the perpendicular angle requirements between L, W, and T. The theoretical and experimental values of L, W, and T (Table 2) generally agree within measurement uncertainty [11]. All sorts of empirical characterizations of aggregates using this L, W, and T information, e.g. "flat and elongated" [14] can be easily computed from these quantities.

5. Four kinds of real aggregates: image acquisition and sieve analysis

Using the X-ray CT/spherical harmonic technique, we examined four different kinds of aggregates, denoted: granite (GR), limestone (LS), Indiana (IN), and Arizona (AZ), which had all passed a 25.4 mm sieve and were retained on a 2.36 mm sieve [15–17]. These four kinds of aggregates were intended to

Table 2
Listing the theoretical (computed from the spherical harmonic series) and experimental (measured with digital calipers) values found for the length (L), width (W), and thickness (T) of the three reference rocks

Reference rocks		L (mm)	W (mm)	T (mm)
Rock 1	Theory	77.4	56.3	31.0
	Experiment	77.4	55.2	31.2
Rock 2	Theory	81.5	62.3	29.1
	Experiment	83.0	62.9	28.7
Rock 3	Theory	74.5	58.5	15.6
	Experiment	71.9	57.0	15.3

Table 3

Comparison between experimental (e) and image-based (i) sieve analyses for four kinds of aggregates [GR=granite, LS=limestone, IN=Indiana, AZ=Arizona]

ASTM sieve	GRe	GRi	LSe	LSi	INe	INi	AZe	AZi
25.4 mm	0	0	0	0	0	3	0	0
19.05 mm	2	8	18	32	10	25	0	0
12.7 mm	40	48	66	40	53	48	7	10
9.52 mm	26	22	14	12.6	26	18	61	51
4.75 mm	30	20	3	15	11	5	32	37
2.36 mm	2	2	0	0.4	0	1	1	2

The first column is the sieve size and the rows are the mass percent (e) or volume percent (i) retained on that sieve.

cover a wide range of aggregates commonly used in the U.S. in terms of shape and texture. The GR and LS aggregates, both from Oklahoma, were crushed aggregates. The AZ and IN aggregates were siliceous river gravels and were not crushed [15]. All X-ray CT samples were 100 mm diameter by 200 mm high cylindrical samples of coarse aggregates cast in cement paste. These aggregates were imaged at approximately the same horizontal resolution, 0.2 mm per voxel, but at differing vertical resolutions: GR – 0.7 mm per voxel, LS – 0.8 mm per voxel, IN – 0.8 mm per voxel, and AZ – 0.4 mm per voxel.

Once the spherical harmonic coefficients were generated for several hundred examples of each kind of aggregate, some statistical analysis could be done. A sieve analysis was simulated, since the volume of each particle is known [1]. For a sieve analysis of a single kind of rock, mass fractions are the same as volume fractions if we assume that the relative density of each kind of rock is the same. There is usually some distribution in relative densities [11], but only by an order of 10%, so we neglect that here. The only choice to be made when constructing a sieve analysis is how to devise a length from the known volume of each non-spherical particle. We chose to compute the equivalent spherical diameter. If V is the true volume of the aggregate, then D, the equivalent spherical diameter, is given by $D=(6V/\pi)^{1/3}$. An experimental sieve analysis of the kinds of particles that went into the sample was also performed.

Table 3 shows a comparison between experiment and simulation for the four kinds of aggregates in terms of mass percentage retained at each of six sieve sizes. There is good qualitative agreement in the overall distributions among sieve sizes, although there are some significant disagreements within individual bins. There are two primary reasons for these differences. The first is that the equivalent spherical diameter
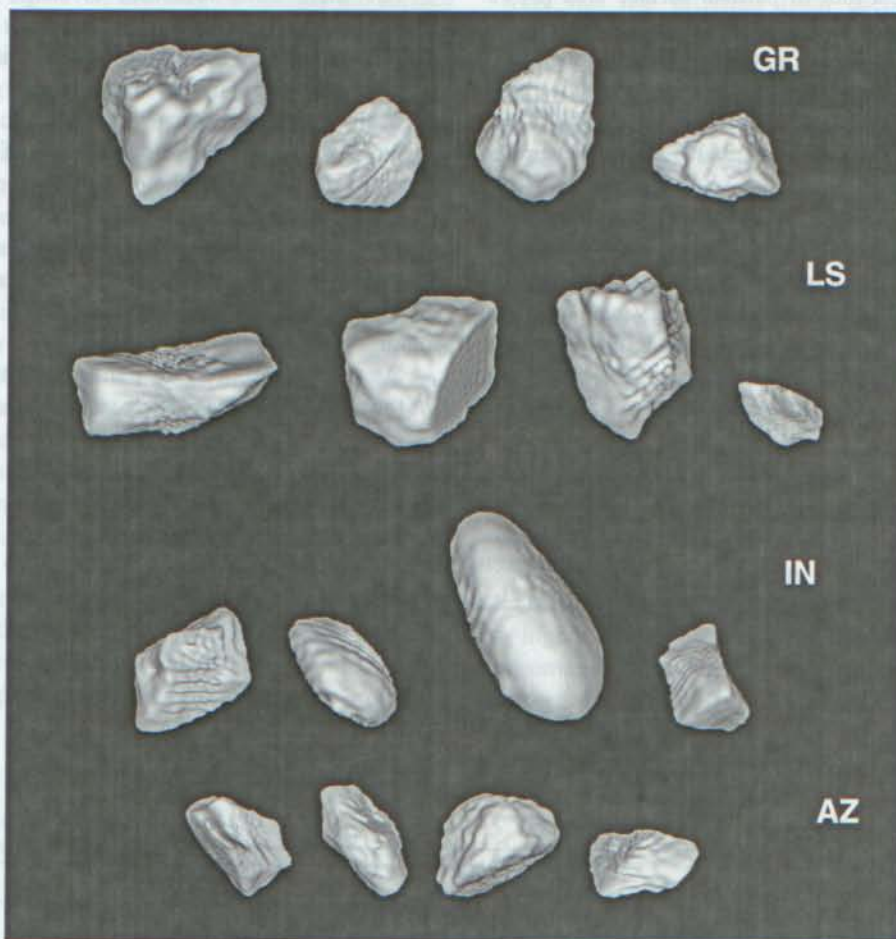

Fig. 3. VRML images of four typical particles each selected from the four different kinds of aggregates studied in this paper. The relative aggregate sizes are approximately accurate. Note that the AZ particles are all about 12 mm in size.

based on particle volume is not exactly the same as the effective length of a square-holed sieve. The second reason is that the image-based analysis only uses a few hundred particles. So, especially for sieves for which the particle numbers were small (larger size particles), there can be a high degree of statistical fluctuation.

Fig. 3 shows four aggregates each of GR, LS, IN, ands AZ. The images were taken from VRML images. The sizes have been adjusted to approximate the scaling of the equivalent spherical diameter.

6. Four kinds of real aggregates: numerical shape analysis

This section gives examples of different ways the spherical harmonic coefficients can be used to analyze the shape of the four kinds of coarse aggregates studied above. A recent paper by Masad et al. [18] contains other ways to use the spherical harmonic coefficients to quantitatively analyze the shape of particles. The most effective way to use the spherical harmonic coefficients to quantitatively analyze shape is still an active topic of research.

Since real aggregates are not spherical, how does one show the non-sphericity of real aggregates and the differences in non-sphericity between aggregates? In sedimentary geology [19], this is done by making a plot of particle surface area (S) vs. particle volume (V), which can both be computed from the spherical harmonic analysis [1]. Fig. 4 shows these plots for the GR aggregates. Clearly the data for the GR aggregates lie above the theoretical line for spheres, $S=(36\pi)^{1/3}V^{2/3}\approx4.84V^{0.67}$, so that the GR aggregates are non-spherical by this measure of shape.

A function of the form $S=aV^b$ was fit to each set of aggregate data. Values of a and b, along with the R^2 factor obtained in each case, are summarized in Table 4 for the four kinds of aggregates. The exponents agree very well with the ideal value of 2/3, given that the uncertainties in the exponents are estimated to be at least ±0.03. The value of 2/3 comes from surface area being a 2-D quantity and volume a 3-D quantity,

Table 4
Results of fitting the surface area vs. volume plots for the different kinds of aggregate types studied, where the fitted function was $S=aV^b$

Aggregate type	Multiplicative factor "a"	Exponent "b"	R^2
GR	8.1	0.63	0.99
LS	7.5	0.64	0.997
IN	8.6	0.62	0.99
AZ	9.1	0.61	0.98

hence 2/3=2÷3. The dimensionless prefactors, however, seem to differ by more than the uncertainty, which is estimated to be about ±0.5, based on the accuracy of the shape reconstruction process [1].

Consider other shapes, like cubes or ellipsoids. For a cube, a highly faceted but equi-axed "rock", $a=6$. For an oblate ellipsoid with dimensions $5\times5\times1$, $a=7.7$. For a prolate ellipsoid of revolution with dimensions $1\times1\times5$, $a=6.6$. In Table 4, all of the prefactors for the aggregates studied are significantly greater than 6, the value for a cube, and are actually greater than the values for the oblate and prolate ellipsoids. These higher values must be due to the aggregates' random shape, and possible the finer scale roughness of their surfaces compared to the mathematically smooth cube and ellipsoid.

Are there other measures of shape that will distinguish between different kinds of aggregates [20], especially for aggregates that are thought to perform differently due to shape differences? This is an open-ended question, but some preliminary answers can be given, since spherical harmonic techniques [1] allow the calculation of mean curvature, the moment of inertia, and the maximum linear extent of a particle in any three orthogonal directions [11], along with any other measure that can be defined on the surface. Empirical measures like "flat" and "elongated" can also be computed [21]. Some of these will perhaps serve to further distinguish particle shape.

As an example of another shape measure, Fig. 5 shows plots of the ratio of the true particle surface area to the surface area of
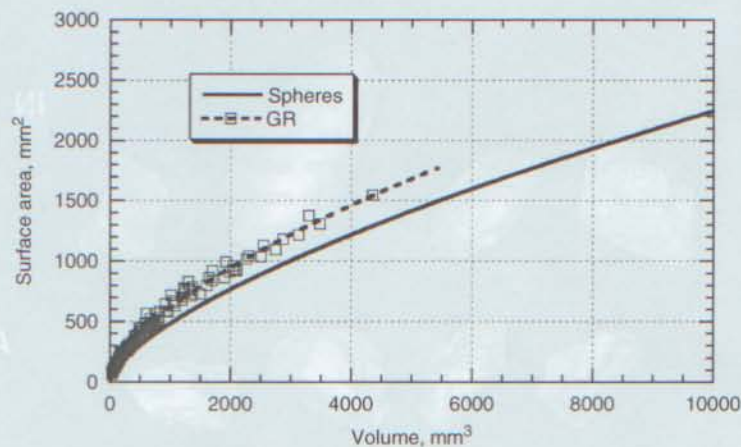

Fig. 4. Plot of surface area, as computed from the spherical harmonic series for each rock, vs. the volume as taken from the original digital image, for the granite (GR) aggregates studied. The solid line is the analytical surface area vs. volume relationship for spheres, $S=(36\pi)^{1/3}V^{2/3}\approx4.84V^{0.67}$. The dashed line is a fit of the form $S=aV^b$ (see Table 4).
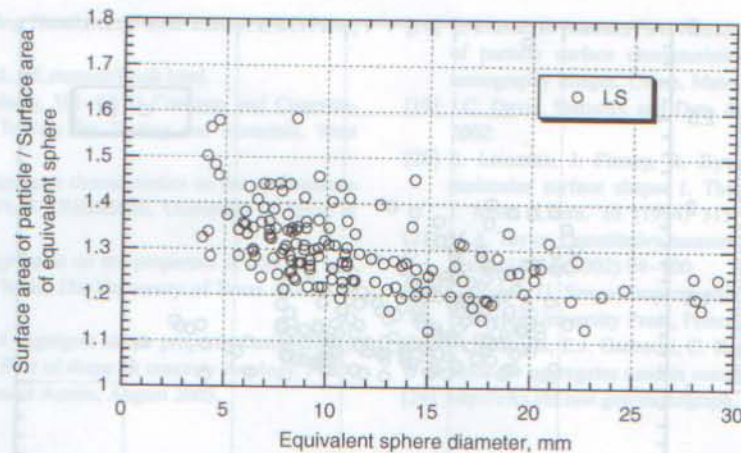
Fig. 5. Plots showing the ratio of the true particle surface area to the surface area of the equivalent sphere, vs. the diameter of the equivalent sphere, for the LS aggregates.

the equivalent sphere, vs. the diameter of the equivalent sphere, for the LS aggregates. A constant value of one for this ratio is only obtained for a spherical particle, and since the sphere is the minimum surface area particle for a given volume [22], increasing non-sphericity is shown by higher values of this parameter. In Fig. 5, the data are more randomly distributed than the points in Fig. 4. However, this may be because the surface area ratio is more sensitive to surface roughness and other features than to the basic shape of the particle. There seems to be a trend towards higher values of this dimensionless ratio for smaller equivalent spherical diameters, indicating that the smaller particles are more non-spherical than are the larger aggregates.

As was mentioned for the three reference rocks, the spherical harmonic coefficients can be used to compute the L, W, and T parameters. It was not possible to remove the rocks from the cement paste matrix and perform direct measurements. For the four aggregates, Table 5 shows the average values of L/T and W/T for all the aggregates studied. The one standard deviation uncertainties come from an average over all particles. The standard deviation presumably comes from actual randomness among rocks and any size dependence of the L, W, and T parameters as was hinted at for other shape quantities in Fig. 5. The column marked "L/W" shows the ratio of the average value of L/T to the average value of W/T. If this value were close to 1, and both L/T and W/T were greater than 1, then the particles would tend to be more oblate. If the L/W value were significantly larger than 1, and W/T was close to 1, then the particles would tend to be more prolate in shape.

Two-dimensional shape histograms can be defined for aggregates [11], which can be helpful in seeing how prolate or how oblate an aggregate type is. However, the scans were not of high enough resolution and not enough rocks were scanned in order to give accurate shape histograms. Table 5 appears to indicate that the shapes of the four kinds of coarse aggregates were not too different from each other. These were all aggregates obtained from commercial suppliers, so that they had to pass various standard tests to be marketable. This may be the reason for the shape similarity of these aggregates. The performance of these aggregates in fresh and hardened concrete has been studied extensively [15–17]. Quantitatively connecting the shape data to well-known theories of how shape affects rheology needs further study [4].

A final method concerns the moment of inertia tensor [1,21], which relates the rotational response of the particle to an applied torque, in a way similar to how mass relates the translational response to an applied force. If we take the trace of the moment of inertia tensor, divided by three, and divide by the moment of inertia of the equivalent sphere, this ratio is a measure of the non-sphericity of the particle, since it is equal to a constant value of 1 for a spherical particle. One-third times the trace of the moment of inertia tensor for a sphere is $2/5R^2 = 1/10D^2$, where R is the radius and D is the diameter of a sphere. Fig. 6 shows graphs of this quantity for the IN aggregates. There is a lot of noise in the graph, but just like in Fig. 5, there seems to be a higher value of non-sphericity as the particle diameter becomes smaller. The moment of inertia tensor is a subject of further study [11,21].

7. Summary and future work

This paper has presented an effective procedure for acquiring aggregate shape data from X-ray computed tomography (CT), including sample preparation, 2-D and 3-D image analysis, 3-D particle reconstruction from 2-D slices, and error correction to eliminate artificially mis-shaped particles. VRML images can be easily generated for each particle, and are useful for qualitative examination and comparison to real images. Real

Table 5
A list of the average and standard deviation of the L/T and W/T values for the AZ, GR, IN, and LS aggregate types studied

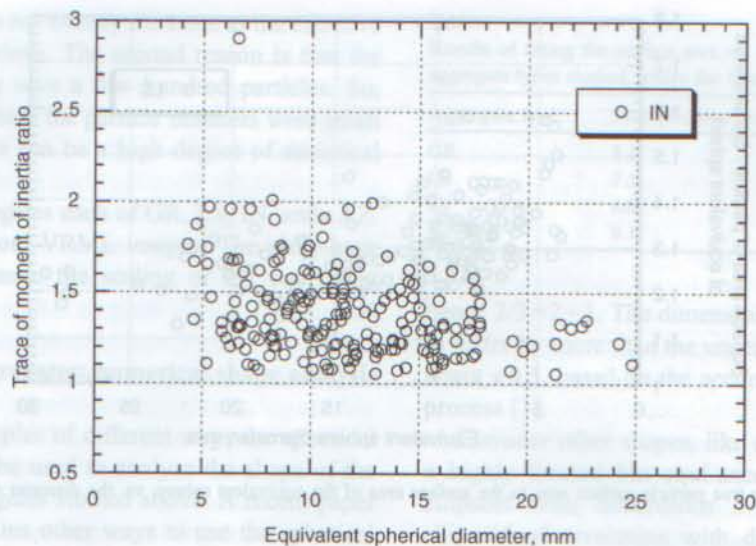| Aggregate type	L/T	W/T	L/W
AZ	2.52 + 0.83	1.74 ± 0.50	1.45
GR	2.12 ± 0.54	1.53 ± 0.38	1.39
IN	2.20 ± 0.62	1.66 ± 0.46	1.33
LS	2.12 ± 0.53	1.51 ± 0.36	1.40

Fig. 6. The ratio of the trace of the actual moment of inertia tensor to the moment of inertia of the equivalent diameter sphere for the GR and LS aggregates.

reference rocks were used to assess uncertainties in the whole process. Results were displayed for four different kinds of aggregates, illustrating the sorts of shape analysis possible using complete 3-D shape information.

There is a wide array of aggregates used in the U.S. and an even greater range of material worldwide. It is known from sedimentary petrology that characteristic shapes can often be qualitatively predicted from knowledge of geological deposits and geomorphological processes. However, these methods cannot give precise numerical information. But we cannot image them all. A research goal is, using information obtained from a statistical sample of aggregates (100s to 1000s), to be able to statistically and realistically generate aggregates based on morphological descriptions [23]. This goal requires a solid and detailed numerical foundation on which to base such statistical predictions. Hence, there is a need for imaging more kinds of aggregates, in order to expand our database and to develop correlations between spherical harmonic coefficients and physical shape as well as standard shape descriptors such as ASTM D-4791 [14]. Examining mathematical differences between crushed and naturally rounded aggregates would probably be instructive. The large amount of data that the spherical harmonic coefficients represent open up many possibilities for mathematical analysis of aggregate shape. A few possibilities were discussed in this paper, but many more need to be studied [11].

Expanding the aggregate database in the Virtual Cement and Concrete Testing Laboratory (VCCTL) will also allow better prediction of a wider range of concrete mixes. The VCCTL is an integrated software package for predicting the properties of concrete from knowledge of the basic ingredients, hydration chemistry, and curing conditions [24]. Having basically complete 3-D shape information for many aggregates will give us an unprecedented ability to realistically model the structure and predict the properties of concrete.

References

[1] E.J. Garboczi, Three-dimensional mathematical analysis of particle shape using X-ray tomography and spherical harmonics: application to aggregates used in concrete, Cem. Concr. Res. 32 (2002) 1621–1638.

[2] J.F. Douglas, E.J. Garboczi, Intrinsic viscosity and polarizability of particles having a wide range of shapes, Adv. Chem. Phys. 91 (1995) 85–153.

[3] E.J. Garboczi, K.A. Snyder, J.F. Douglas, M.F. Thorpe, Geometrical percolation threshold of overlapping ellipsoids, Phys. Rev., E 52 (1995) 819–828.

[4] E.J. Garboczi, J.F. Douglas, Intrinsic conductivity of objects having arbitrary shape and conductivity, Phys. Rev., E 53 (1996) 6169–6180.

[5] M.L. Mansfield, J.F. Douglas, E.J. Garboczi, Intrinsic viscosity and the electrical polarizability of arbitrarily shaped objects, Phys. Rev., E 64 (2001) 61401–61416.

[6] E.J. Garboczi, J.F. Douglas, R.B. Bohn, The intrinsic elastic moduli of rectangular parallelepiped inclusions over a modest range of shape and a large range of property contrast, Special Issue of Mech. of Materials. (in press).

[7] A.C. Kak, M. Slaney, Principles of Computerized Tomographic Imaging, SIAM, Philadelphia, 2001.

[8] E.J. Garboczi, Tying together theory and tests via virtual testing, Stone, Sand, and Gravel Review, January/February 2006, pp. 10–11, Available in Electronic Monograph, http://ciks.cbt.nist.gov/monograph/, Part I, Chapter 10, Section 6.

[9] D.W. Luerkens, Theory and Application of Morphological Analysis: Fine Particles and Surfaces, CRC Press, Boca Raton, Florida, 1991.

[10] D.W. Ritchie, G.J.L. Kemp, Fast computation, rotation, and comparison of low resolution spherical harmonic molecular surfaces, J. Comp. Chem. 20 (1999) 383–395.

[11] M.A. Taylor, E.J. Garboczi, S.T. Erdogan, D.W. Fowler, Some properties of irregular particles in 3-D, Powder Technol. 162 (2006) 1–15.

[12] J.C. Russ, The Image Processing Handbook, Fourth edition CRC Press, Boca Raton, Florida, 2002.

[13] www.web3d.org/resources/vrml_ref_manual/Book.html.

[14] ASTM Annual Book of Standards, Vol. 04.03 Concrete and Concrete-Making Materials, American Society for Testing and Materials, West Conshohocken, PA, 1999.

[15] P. Quiroga, The effect of the aggregate characteristics on the performance of Portland cement concrete, Ph.D. Dissertation, University of Texas at Austin, December 2003.

[16] S.T. Erdogan, The effect of aggregates on the properties of concrete and proportioning methods, M.S. Thesis, The University of Texas at Austin. August 2003.

[17] S.T. Erdogan, Determination of aggregate shape properties using X-ray tomographic methods and the effect of shape on concrete rheology, Ph.D. Dissertation, University of Texas at Austin, August 2005.

[18] E. Masad, S. Saadeh, T. Al-Rousan, E.J. Garboczi, D. Little, Computations of particle surface characteristics using optical and X-ray computed tomography images, Comp. Mater. Sci. 34 (2005) 406–424.

[19] J.C. Davis, Statistics and Data Analysis in Geology, 3rd edition Wiley, 2002.

[20] S. Leicester, J. Finney, R. Bywater, A quantitative representation of molecular surface shape: I. Theory and development of the method, J. Math. Chem. 16 (1994) 315–341.

[21] M.A. Taylor, Quantitative measures for shape and size of particles, Powder Technol. 124 (2002) 94–100.

[22] G. Polya, G. Szego, Isoperimetric Inequalities in Mathematical Physics, Princeton University Press, Princeton, 1951.

[23] M. Grigoriu, E.J. Garboczi, C. Kafali, Spherical harmonic-based random fields for aggregates used in concrete, Powder Technol. (in press).

[24] http://ciks.cbt.nist.gov/monograph, see button for VCCTL.